

Fundamentals and Similarity Transformations of Vectored Aircraft

Benjamin Gal-Or*

Technion—Israel Institute of Technology, Haifa 32000, Israel

Fundamental concepts and new similarity transformations for emulating rapidly rotating-translating, poststall (PST), thrust vectoring flight controlled (TVFC) aircraft are defined and employed to design scaled-model flight tests aimed at proof of concept, maximization of agility during PST supermaneuvers, and the estimation of g loads on the pilot during such maneuvers. Deficiencies vs compromises regarding drop and powered model methodologies are defined, and a basic rule regarding maximization of jet-deflection rates is formulated. The new similarity laws are combined with standard agility comparison maneuvers (SACOM) conducted with powered, PST, TVFC F-15, F-16, and F-22 models. The new SACOM methodology helps define safe vs forbidden pilot-airframe, space-time domains that infer far-reaching safety vs combat-agility consequences for future fighters, including tailless vectored designs.

Nomenclature

b	= reference span, m
C_D	= drag coefficient, dimensionless
C_{D8}	= nozzle discharge coefficient, dimensionless
C_{fg}	= nozzle thrust coefficient, dimensionless
C_L	= lift coefficient, dimensionless
C_m	= pitching moment coefficient, dimensionless
C_{mo}	= basic pitching moment coefficient, dimensionless
C_{mq}	= pitching moment derivative with respect to pitch rate, 1/rad
C_n	= yawing moment coefficient, dimensionless
C_x	= longitudinal force coefficient, dimensionless
C_y	= side force coefficient, dimensionless
C_z	= normal force coefficient, dimensionless
c	= reference mean aerodynamic chord, m
D	= the distance from thrust vectoring (TV) nozzle exit to aircraft C_{py} , m
D^*	= the distance from TV nozzle exit to aircraft center of gravity, m
D_{cpy}	= the drag operating at C_{py} , kgf
G_z, G_y, G_x	= g loads on pilot or aircraft in the respective body-axis coordinates, m/s^2
I_x	= moment of inertia about the roll axis, $kg\cdot m^2$
I_y	= moment of inertia about the pitch axis, $kg\cdot m^2$
I_z	= moment of inertia about the yaw axis, $kg\cdot m^2$
L	= linear scale factor, m
M	= vehicle mass, kg; also Mach number
\dot{M}	= nozzle air mass flow rate, kg/s
q	= pitch rate, rad/s
\bar{q}	= dynamic pressure, employed with reference area s , $(\frac{1}{2})\rho V^2$, N/m^2
r	= yaw rate, rad/s; radius, m
s	= reference aircraft surface area for dynamic pressure/force calculations, m^2
T	= actual, net, thrust, kgf; also temperature
T_i	= ideal isentropic, net, thrust, kgf

T_v	= pitch thrust vectoring component, kgf
$T_{x,y,z}$	= thrust-vectored components in the body-axis x, y, z coordinates, kgf
t	= time, s
V	= true airspeed, m/s, or volume
W	= flying vehicle weight, kgf
α	= angle of attack; also AoA, deg, or rad
β	= angle of sideslip, deg, or rad
δ_v	= effective pitch thrust-vectoring angle, may be a differential angle; deg, or rad
δ_y	= effective yaw thrust vectoring angle, may be a differential angle; deg, or rad
$\bar{\rho}$	= average vehicle density, kg/m^3

Introduction

TRADITIONALLY, jet engines have been considered to have little influence on flight-control systems, flight ceiling, and maximized combat agility. They were confined to provide brute, unvectored, forward force. The required moments for maneuverability and controllability were reserved for aerodynamic control surfaces, which are, a priori, limited by external flow regimes, and hence, by the so-called stall barrier.

This thinking has totally ignored the unprecedented control potentials of engine forces/moments, especially beyond the so-called stall limit, i.e., during "impossible" PST, rotating-translating maneuvers at extremely high pitch, yaw, and roll rates, where "well-established" aerodynamic concepts and flight control means fail. Consequently, in the past aerodynamicists tended to develop flight control means with no role for jet thrust deflection and deflection rates. However, the increasing demands on PST agility, higher altitudes, and supermaneuverability have recently begun a radical change in these attitudes,^{1,2} agility definitions,³ and scaling methodologies.⁴⁻¹⁵ It was realized that there are no unified framework and criteria to define and quantify the new problems properly.

Therefore, new integrated criteria involving dynamic and vectoring-propulsive scale factors and PST-TVC yardsticks of effectiveness have been developed by this jet laboratory, apparently from no verifiable base of flight data in the deep PST domain. In turn, such attempts to revolutionize the mode of thinking of propulsion, aerodynamic, system design, and flight-control engineers, may change the basic approach to aeronautical engineering education, theories, and practice.

Unless otherwise stated, TVFC refers below to "complete" roll-yaw-pitch TVFC, i.e., to a new technology which opens the road to the design of tailless vectored fighters.^{1,4}

Received Jan. 24, 1992; revision received Feb. 1, 1993; accepted for publication Feb. 1, 1993. Copyright © 1993 by B. Gal-Or. Published by the American Institute of Aeronautics and Astronautics, Inc., with permission.

*Professor and Head, Jet Laboratory.

This article reassesses PST agility concepts and the new domains of future TVFC aircraft. In light of new needs and concepts it re-examines conventional theories, laboratory, and flight-testing methodologies that are currently required to design, construct, and flight-test properly scaled, powered, PST-TVFC models aimed at the maximization of PST combat effectiveness.

Reassessment of Poststall Agility Concepts

The future availability of PST-TVFC fighters, helmet-sight-aiming systems, and all-aspect missiles, requires reassessment of the optimal balance between aircraft and missile abilities. Whatever the balance, high-performance fighter aircraft will gradually be based on improved TVFC maneuverability/controllability.¹

In offensive engagements it means the ability to rapidly rotate the nose in the general direction of the enemy to minimize weapon's flight-path to target. This minimum-time rule increases kill-ratio probabilities¹ to destroy the target prior to its launching its weapon, for otherwise the probabilities of mutual destruction increase dramatically. Moreover, the new PST-TVFC technologies generate significant key factors in advancing defensive, safety, takeoff/landing, and air-to-ground capabilities.¹ For instance, in defensive engagements it means dramatic increases of survivability, using, e.g., very rapid, unconventional pure sideslip rotations/translations, without banking.²⁻⁴

Replacing conventional flight control (CFC) trimming by TVFC jet trimming cuts drag in subsonic and supersonic flight, while the improved survivability and combat effectiveness may reduce fleet size with respect to expected missions/threats.¹⁻³ Such new capabilities include stealth tailless designs or aircraft with reduced aerodynamic tail surfaces.⁴ Consequently, the introduction of PST-TVFC technologies requires reassessment of most conventional mission and design concepts, and the generation of new inertia, vectoring, propulsive, aerodynamic, control, pilot-flyer, aeroelastic, and atmospheric similarity laws.

New Flight Domains

Figure 1 defines the new domains of transient PST rotations and TVFC-enhanced flight-control/envelopes. It schematically shows how TVFC power decreases with altitude, while increasing with speed up to a maximum value. Such potentials are represented by the T/W lines in the figure. Transitions from beyond visual range (BVR) to within visual range (WVR) engagements increase pilot's needs for transient, TVFC-enhanced, rotations-translations in air-to-air and in air-to-ground tactics. Therefore, TVFC becomes a key combat element, especially in close-in combat engagements, in air-to-ground operations, in gaining STOL/safety qualities, in reducing optical, IR and radar signatures, and in reducing trim drag/fuel

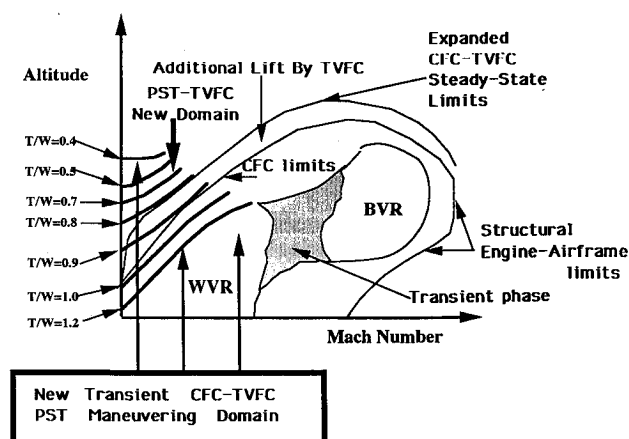


Fig. 1 New domain of poststall thrust-vectoring maneuvers.

consumption.¹ The use of downpitch TV may increase direct and supercirculation-generated lift,² thereby slightly expanding the upper flight envelope, as depicted.

We therefore assert that in future aerial combat, once the engagement has closed to WVR, even under multitarget situations, PST-TVFC effectiveness becomes a critical capability to win and survive. Dramatic increases in performance and survivability in revolutionary air-to-ground tactics are also expected.^{2,3,15} Hence, the fundamental concepts and efficiencies/limitations of conventional vs PST-TVFC aircraft must be well-formulated/flight-tested by means of dynamically scaled prototypes, using proper similarity transformations. Exploring the entire PST-TVFC domain by full-scale TVFC aircraft is prohibitive for safety, cost, time, and limited performance reasons.

Debate over Proper Similarity Transformations

The debate began in September 1992 at both DARPA and the Flight Dynamics Directorate at Wright-Patterson AFB, following an invited lecture on PST-TVFC. Re-examining the design definition, mission, and performance of the new TVFC, X-31 experimental fighter aircraft, and its emulating, 1/3th-scaled NASA drop-model, the debate centered on such fundamental questions as "How should combat-effective, PST-TVFC-agility be defined and measured?"; "Can NASA's unpowered X-31 drop model emulate rapidly rotating-translating, X-31 PST-TVFC-agility?"; "Can previous, USAF-NASA, unpowered, free-flying and drop models¹¹⁻¹⁴ emulate agility during PST-TVFC-induced rotational-reversing rates, when CFC fails and rapidly deflecting jets affect combat effectiveness?"

Currently, there is a general agreement on the importance of "PST-TVFC-relevant similarity rules," and a general disagreement on which models and which similarities to apply, at what priorities and compromises, and under what physico-engineering presuppositions and formulations.

The first question has already been treated in Ref. 3, which shows that four PST-TVFC agility components should be defined and measured during PST-TVFC rotational-reversals, and that TVFC authority should be maximized when CFC fails (Figs. 2 and 3). The other questions are assessed below.

Uncovering and Maximization of a Net Agility

With the rapid advance of new technologies, engagement times get shorter, and the minimization of inherent delay

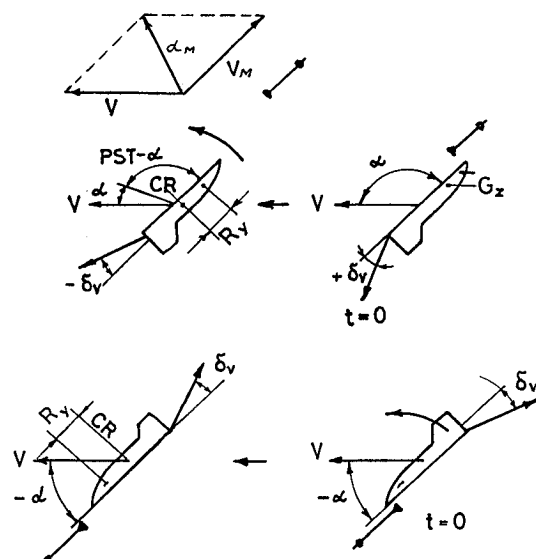


Fig. 2 Maximization of TV-moments and rates at the reversal point of positive and negative 'Cobra' maneuvers. (Note dangerous interactions with high-AoA launched missiles. V_M = missile's initial velocity vector whose magnitude increases with launch-rail length.)

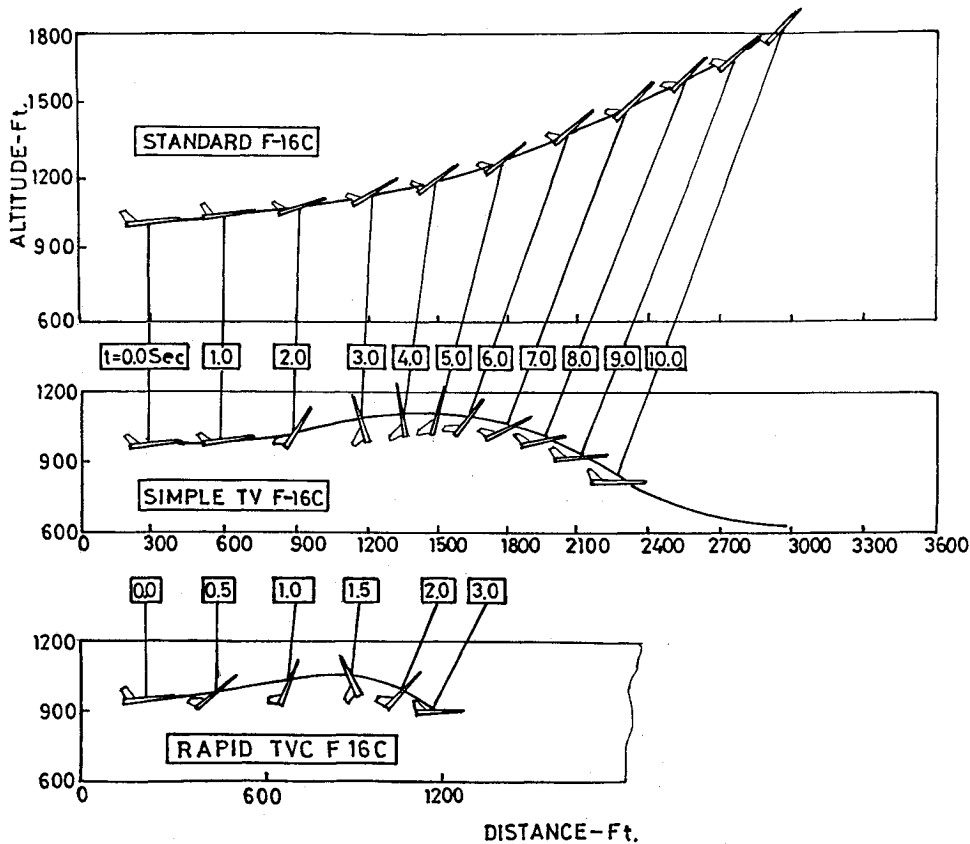


Fig. 3 Rule 1: maximum jet-vectoring rates should equal conventional deflection rates. Upper figure: conventional pitch rate at maximum pilot tolerance and restricted maximum alpha. Lower figure: at low speeds, the faster the maneuver, the safer it becomes for a pilot located near the center of rotation. Midfigure: a slow PST-TV-induced turning rate is less combat effective.

times of TVFC nozzles, pilot, and TVFC hardware becomes more critical to combat effectiveness. Hence, to predict PST agility by flying powered, properly scaled TVFC models, we first define aircraft gross agility (AGA) as

$$\text{AGA} = \text{MGA}[\text{DSF}]F_1[\text{Turb.-MLEM}]F_2[\text{PDT/FDT}] \times F_3[\text{A-IFPC}]/[\text{M-IFPC}] \quad (1)$$

where MGA is the scaled model gross agility, DSF the dynamic scale factors, to be defined below, $F_1[\text{Turb.-MLEM}]$ the functions of "turbulence noise and maximum likelihood estimation method," $F_2[\text{PDT/FDT}]$ the ratio of pilot to flyer delay times during actual, in-flight SACOM, and $F_3[\text{A-IFPC}]/[\text{M-IFPC}]$, the control functions relating aircraft integrated flight propulsion control (IFPC), to model-IFPC.^{3,4}

Without stating it, Eq. (1) assumes that each vehicle is characterized by a hidden, bona fide, net agility—a basic combat-technological quality that the propulsion/airframe designer and the theoretician both want to uncover and maximize.

Radius of Gyration

The inertia tensor, I_{ij} ($i, j = 1, 2, 3$, or x, y, z) can be divided into an inertial tensor relative to the center of mass (c.m.) of the aircraft, and an inertia tensor relative to another point of reference. Hence, the quantities associated with it—principal axes, principal moments, etc.—are relative to a particular point of reference.

If the reference point is shifted from the c.m. of the aircraft to another point, as is required for improved understanding of PST-TVFC rotational agility, these quantities change accordingly.

The combined translational-rotational dynamics of, e.g., pure-pitch SACOM,³ may similarly be split into two separate

formulations, one purely translational and the other purely rotational about a reference point.

To simplify the formulations of rigid-body rotational dynamics and flight tests of PST-TV vehicles, we first examine the radius of gyration, a fundamental quantity which is directly related to the moments of inertia. For instance, the radius of gyration around the pitch axis of the rotating PST-TV aircraft or model R_y is defined by

$$R_y = (I_{yy}/M)^{0.5} \quad (2)$$

where M is the mass of the flying vehicle.⁷

Flight tests conducted by this laboratory employ the radius of gyration formulation to extract improved understanding of pilot tolerances in dynamically scaled, yaw-pitch, or roll-yaw-pitch PST-TVFC F-15, F-16, and F-22 fighter aircraft upgrades (Table 1).

The main question is, therefore, what is a dynamically scaled PST-TVFC model, and in particular, what should be its weight and moments of inertia with respect to the emulated full scale aircraft. For that purpose one must transform aircraft-to-model (AtM) moments of inertia and mass, as shown below.

Subscale Model to Full-Scale Aircraft Similarity Laws

Equations (1) and (2) require a prudent integration of a number of similarities between flying, rotating-translating, PST-TVFC aircraft, and the emulating powered model. There are 10 main similarities involved: SACOM, geometric, inertial, vectoring, propulsive, aerodynamic, IFPC, pilot/flyer, atmospheric, and aeroelastic. Maintaining stick command and DSF similarities under the same SACOM³ is a basic similarity requirement. Hence, unpowered, free flying, or drop models cannot emulate PST-TVFC performance. Yet, even with properly scaled powered models, one cannot maintain complete similarity in materials and servo-actuator IFPC systems. It is

Table 1 Emulations of maximized TVC-induced pitch agility^a

	Actual flight	DIP Adjust	Full-scale
^b Max CFC-TVC pitch rate, deg/s	175	182	69
^b Time to max pitch rate	0.55	0.86	2.3
^b Max CFC-TVC G_z , m/s ²	71	41	41
^b Time to max G_z , s	0.5	1.0	2.6
^b Max CFC-TVC G_x , m/s ²	-17.6	-16.5	-16.5
^b Max CFC-TVC alpha, deg	73	93	93
^b Initial level speed, m/s	32	32	85
^c CFC max pitch rate, deg/s	95	53	20
^c Time to max CFC pitch rate, s	0.6	0.87	2.3
^c Corresponding CFC G_z , m/s ²	44	22	22
^c Time to corresponding conventional G_z , s	0.5	1.0	2.6
^c Corresponding CFC G_x , m/s ²	-8.3	-8.8	-8.8
^c Max CFC-TVC alpha, deg	32	32	32
^c Initial level speed, m/s	32	32	85
^d Max positive TVC- q , deg/s	70,75,75	100	38
^d Time to max positive TVC- q , s	1.6	1.0	2.6
^d Max positive G_z , m/s ²	46,42,39	26-31	26-31
^d Corresponding CFC G_x , m/s ²	-5.5	-5.8	-5.8
^d Max CFC-TVC alpha, deg	40	65	65
^d Initial level speed, m/s	34	34	90
Mass, kg	14	44	15,161
I_{xx} , kg-m ²	0.88	2.69	45,257
I_{yy} , kg-m ²	4.92	13.94	234,213
I_{zz} , kg-m ²	5.42	15.48	260,237
Radius of gyration, R_x , m	0.25	0.25	1.73
Radius of gyration, R_y , m	0.59	0.56	3.93
Radius of gyration, R_z , m	0.62	0.59	4.14

^aActual flight refers to measured flight data of roll-yaw-pitch-TVC, $\frac{1}{4}$ -scale, F-15 prototype, taken from Ref. 15. The values were recorded 20 times per second on-board a 14 kg, $T = 8$ kgt, 7% static stability margin. CFC-TVC F-15 model performing pure-pitch-PST-SACOM at sea level, starting from level flight.

^bValues are from a combined, CFC-TVC, pitch-SACOM (pp. 58, 60).

^cValues are from a conventional (elevator-only) command. Reference 15, pp. 55, 57.

^dValues are from a vectoring-only pitch command. Reference 15, pp. 61, 63.

possible, however, to measure F_2 [PDT/FDT] and F_3 [A-IFPC]/[M-IFPC] during a well-defined SACOM.^{3,4,15}

Corrected Geometric-Aerodynamic-Inertial Similarities

As with wind-tunnel models we first request a strict geometrical similarity between aircraft and model to roughly approximate aerodynamic similarity beyond a certain high Reynolds number value for both model and aircraft, namely, we first require that for each external vehicle configuration skin coordinate, $i = 1, 2, 3$, or x, y, z

$$\frac{(dx)_A}{(dx)_M} = L \quad (3a)$$

or

$$r_A = Lr_M (L > 1)$$

where the subscripts M and A refer to model and full-scale aircraft, L is a constant scaling factor, and r a vehicle's symmetric external-shape radius. Hence, geometric similarity (3a) dictates that, say

$$c_A = Lc_M, \quad s_A = L^2s_M \quad (3b)$$

Various free-flying and drop models were designed, constructed, and flight tested previously by NASA and the USAF.¹¹⁻¹⁴ The transformation employed by USAF and NASA teams in designing the required dynamic similarity between full-scale aircraft and model is

$$I_M = I_A L^{-5} [\rho_{aL}/\rho_{aSL}]^{-1} \quad (3c)$$

where ρ_{aL}/ρ_{aSL} is the ratio of local air density to that of sea level. That air density ratio was assumed to provide "Froude number scaling and altitude scaling."^{12,13} Therefore, all moments-of-inertia constructed into the USAF and NASA models obeyed transformation (3c).

As derived and proved by Eq. (4) below, the ratio of moments-of-inertia transformations is:

$$\begin{aligned} I_M &= \int_{M_A} r_M^2 dM_M = \bar{\rho}_M \int_{V_A} L^{-2} r_A^2 L^{-3} (dx)_A \\ &= \bar{\rho}_M L^{-5} \int_{V_A} r_A^2 (dx)_A = I_A L^{-5} (\bar{\rho}_M/\bar{\rho}_A) \end{aligned} \quad (4)$$

where, for the full-scale aircraft, the integrated (averaged) moment-of-inertia components are defined by

$$\int_{V_A} r_A^2 (dx)_A = I_A/\bar{\rho}_A \quad (5)$$

where M is mass and V volume.

Provided transformation law (4) is obeyed, the scaled flying models are subject to

$$(G_i)_M = (G_i)_A \quad (6)$$

The well-known transformation (6) means that, under all dynamic similarity flight restrictions subject to Eqs. (1-5), the "g loads" acting on the pilot and airframe are the same as those monitored by the flying "similar" model during a similar SACOM (Table 1 and Refs. 3 and 15). Following these

requirements, Newton's second law provides two additional, well-known transformations:

$$V_A = V_M(L)^{1/2} \quad (7)$$

[SACOM time for dynamically scaled model]

$$= [\text{full-scale time}](L)^{-1/2} \quad (8)$$

The vehicles density ratio $\bar{\rho}_M/\bar{\rho}_A$ in transformation (4) is calculated from two weight measurements: of model and full-scale vehicle, and the relationship

$$\begin{aligned} W_M &= Mg = g\bar{\rho}_M \int_{V_A} (dx_i)_M = g\bar{\rho}_M L^{-3} \int_{V_A} (dx_i)_A \\ &= W_A L^{-3} (\bar{\rho}_M/\bar{\rho}_A) \end{aligned} \quad (9)$$

Substituting (4) and (9) in (2), one obtains

$$(R_y)_A = L(R_y)_M \quad (10)$$

Equations (4)–(10) are general fundamental physical similarity transformations. Each remains valid irrespective of any linear or nonlinear fluid dynamic formulations, or boundary-layer and Froude number simplified models, or other unsubstantiated presuppositions. Hence, these transformations form the basis of our generalized similarity laws and flight-testing methodology.^{1–4,15} Moreover, using (10) and (2), one can introduce the radius-of-gyration methodology to emulate PST-TVFC-induced g loads on the pilots by means of large emulating centrifuges.^{8,9}

Flight Testing via the Similarity Transformations

To illustrate the correct use of the general transformations, one may first examine a pure pitch-SACOM, i.e., a pure flip-up-down, starting from a sustained level flight. The resulting “rotational-reversal-onset,” keeps the vehicle's flight-path approximately horizontal for a short duration (Fig. 3). Now, to maximize PST-TVFC agility, the most critical element is the rapid reversal of the vectoring jet angle to generate the fastest reversal in pitch rotation under PST conditions.^{3,15} This is the ultimate test of PST-TVFC power to maximize functional agility, namely, to minimize “time-to-target-and-recover.”²³ Under these conditions the reversal command generates rotational rate approximated by the pitch component of the equations of motion,¹⁰

$$\dot{q}I_y = \dot{q}sc[C_{mo}(\alpha) + (c/2V)C_{mq}(\alpha)q + D^*C_{fg}(\delta_v)T_i \sin \delta_v] \quad (11)$$

This SACOM reverses the jet direction where the aerodynamic effects are small in comparison with the thrust-vectoring reversing moments. When $\alpha = 90$ and $q = 0$, as an approximation

$$\dot{q} = [D^*C_{fg}(\delta_v)T_i \sin \delta_v]/I_{yy} \quad (12)$$

Substituting Eqs. (3), (4), (7), (8), and (9) in Eq. (11) or Eq. (12), one obtains

$$\dot{q}_M = L\dot{q}_A(\bar{\rho}_M/\bar{\rho}_A)(\rho_{aM}/\rho_{aA}) \quad (13)$$

where, by (8)

$$(\bar{\rho}_M/\bar{\rho}_A)(\rho_{aM}/\rho_{aA}) = 1 \quad (14)$$

Transformation (14) can also be derived from any pitch, roll, and yaw rate functions of model and full-scale vehicles, without neglecting any term, starting from the complete set of six degrees-of-freedom equations of motion.¹⁰ Hence, transformation (14) holds under all CFC, TVFC, and CFC-

TVFC flight conditions. It is a general law that controls all proper subscale models emulating full-scale aircraft performance.

Thrust-to-Weight Ratio and the General Similarity Law

To uncover the fundamental meaning of transformation (14), and to guide its proper use in practice, we first assess the required T/W ratios for both model and aircraft.

Recalling that the engineering units of thrust are [air mass flow rate][velocity], or [air density][flow area][velocity],² we first stress the fact that transformation (14) enforces a thrust-to-weight ratio equality between full-scale aircraft and model. This equality is not imposed, nor presupposed. It is dictated by (14), namely, by the most general equations of motion and transformations (1–10).

Emulating Methodologies: Drop vs Powered PST-TVFC Flying Models

The USAF-NASA free-flying and drop-model methodology^{11–14} provides no TVFC forces/moments, nor any PST-TVFC similarity. While being adjusted for, unpowered models also distort drag via clogged engine inlets.

Three technologies may be employed to power-scaled models that are subject to transformations (1–14); special small jet engines, pulsed jets, or cold propulsion. To satisfy transformation law (14) one may use the small-jet-engine option to construct a model with an average density equal to that of the aircraft and fly it at sea level, or a given altitude, to emulate the performance of a full-scale fighter at the same altitude, under the same SACOM and under the other prerequisites enumerated by 1.

Alternatively, one may use the low-density pulsed or cold propulsion options (the latter may be provided by low-cost ducted fans driven by fast-rotating piston engines), to construct low-density PST-TVFC models that emulate aircraft performance at sea level by conducting SACOM at high altitudes. Since this may not be cost-effective, a compromised methodology is proposed below.

Cost-Effective Methodology for Emulating Maximized PST Agility

A working density iterative process (DIP) for emulating-predicting PST-TVFC agility is illustrated by Table 1. It is based on postflight processing of data by a semi-empirical computer simulation of PST-TVFC agility.¹⁰ The computer inputs for the example shown are actually recorded SACOM commands, IFPC and flyer delay times, recorded initial level speed, measured $\delta_v(t)$, D^* , T_v , T_x , and moments-of-inertia data, as well as known dimensions, weight, $\bar{\rho}_M/\bar{\rho}_A$, thrust, and C_L , C_{mo} , C_{mq} , C_D functions of alpha in the deep PST domain for both model and aircraft. The semi-empirical predictions are first compared with actual flight data. When the agreement is reasonable, “DIP adjust” ratios of “high-to-low density models,” are generated for each variable using the same SACOM and input data, but with higher mass and moments-of-inertia values, to conform with (14), (4), and (9).

“Actual flight” data are then converted by the DIP ratios to DIP adjust data for a high-density model. Then, by means of (4–14), the full-scale data are predicted (Table 1).

For instance, when a powered model with, e.g., $\bar{\rho}_M/\bar{\rho}_A = \frac{1}{3}$ is employed, the low weight allows the use of low-thrust cold propulsion at sea level to emulate aircraft performance at this or higher altitudes, depending on the value of ρ_{aM}/ρ_{aA} dictated by transformation (14).

Our CFC-TVFC F-15 low-density model was designed with a 7% positive static stability.^{4,15} It displays less aerodynamic damping in comparison with the same size-shape, but with a heavier model. That damping is a function of C_{mq} , static stability margin, and the requirement of higher alpha to maintain the same initial level speed for both low- and high-density

models. Other nonlinear effects play increasing roles in the deep PST domain.

To establish verification with a published, or measured, full-scale conventional performance is mandatory for increasing the reliability of predicted full-scale PST-TVC agility. Such a verification is provided in Table 1 by the 20 deg/s max conventional pitch rate. This value is in agreement with known conventional F-15 rates under these emulated conditions. The predicted 69 deg/s pitch rate for a full-scale, upgraded, TVFC F-15 should be considered accordingly.

As long as candidates for TVFC upgrading are a priori prohibited from conducting such rapid rotations-reversals in the deep PST domain, the proposed methodology transformation remains an important research tool. During that period this tool can be used to estimate expected maximized PST-TVFC agility for each new design, including tailless vectored fighters.

In conclusion, the emulation-prediction of full-scale performance by low-density PST-TVFC models appears to be more productive and cost-effective than the use of wind-tunnel or high-density, powered or unpowered/unvectored free-flying and drop models. So far this laboratory is the sole source for emulating-predicting such rapid, yaw-pitch-roll TVFC-induced rotations-reversals in the deep PST domain.

Predicting g Loads on the Pilot

Radius of gyration values are given in Table 1. The values remain approximately invariant by transformations from light to heavy models. By (4), (9), and (14), the DIP Adjust data provide estimations of G_z and G_x data for a high-density model performing the same pitch-SACOM at the same initial speed, but with higher alpha values (Table 1). g Loads expected on a pilot of future full-scale TVC aircraft are, by transformation (6) equal to those displayed as DIP adjust.

Is TVFC Agility Restricted by Pilot Tolerances?

During a SACOM at constant altitude and Mach number, the vertical force on pilot, aircraft, and model becomes, from Eq. (12)

$$C_z = -[C_L(\alpha)\cos \alpha + C_D(\alpha)\sin \alpha] + T_v/\bar{q}s \quad (15)$$

C_z does not change sign when T_v does. To see that, examine how the vectored vertical force depends on the (effective) jet deflection angle variations with SACOM time, viz.

$$T_v = C_{fg}[\delta_v(t)]T_i \sin \delta_v(t) \quad (16)$$

Similarly, during this maneuver, the axial thrust is expressed by

$$T_x = C_{fg}[\delta_v(t)]T_i \cos \delta_v(t) \quad (17)$$

while the yawing vectored thrust remains inoperative, namely

$$T_y = 0 \quad (18)$$

Equations (15–18) are employed to generate a practical SACOM, viz., from level flight initial conditions to level flight end conditions.

The flight tests provide integral “time-to-target-and-recover” data, maximum q rates (reached usually beyond mid-way up and down the flip angle), and maximum “ g onsets on the pilot” beyond the reversal point. The corrected and scaled “ g onsets,” especially the negative ones, quantify the most critical pilot tolerances in a repeatable methodology, while simultaneously providing TVFC-designers with the best yardstick for the maximization of TVFC effectiveness vs unpropitious domains dictated by pilot tolerances (see below).

Such model and/or computer simulations are employed by our team to compare the agility of one design to another.

Numerical and analytical solutions of more general sets (with combined TVFC and CFC, and with particular commands and initial and boundary conditions) are now being investigated while working back and forth between theory and well-controlled SACOM flight tests.

For this purpose, we instrument the dynamically scaled models with three gyros, three accelerometers, and alpha, sideslip, and velocity probes. During the SACOM each variable is recorded 20 times/s on an onboard computer. A synchronized ground computer simultaneously records 40 times/s the TVC commands, and whenever used in the comparisons, the conventional-control commands. The computers and associated software/calibrations/data bases have all been developed towards this aim.

Forbidden Human Space-Time Domains

Situating an hypothetical pilot's head at the center of rotation (CR) (where there are no centrifugal and tangential accelerations during rapid pure pitch-up/down cobra rotations), the normal acceleration on his head is, from Eq. (15)

$$G_z = \{\bar{q}s[C_L(\alpha)\cos \alpha + C_D(\alpha)\sin \alpha] + C_{fg}[\delta_v(t)]T_i \sin \delta_v(t)\}/M \quad (19a)$$

Note that G_z is the same for both the properly scaled model and aircraft, and that it does not change sign when δ_v does (Fig. 2). The hypothetical pilot starts sensing “negative g ” (blood flow into brain) only when, at low speed/drag values, $\bar{q}s[C_L(\alpha)\cos \alpha + C_D(\alpha)\sin \alpha]$ acts to defer crossing into negative g domains, for it introduces a compensating “positive g ” component (blood flow from brain).

Situating the pilot ahead of CR adds positive or negative tangential pitch acceleration, and allows simple calculations of total G_z for a realistic pilot; consequently:

1) Crossing into negative g domains depends on alpha, airspeed, the pilot's distance from CR, q , and the value, sign, and duration of the δ_v command.

2) The higher the speed, the longer the delay time into negative g domains.

3) Contrary to high positive G_z loads, which characterize conventional pitch-up maneuvers, the faster the nose-turning rates, or the shorter the “time-to-target-recover-PST-TV-maneuver,” the more effective and safer it becomes for a pilot situated close to CR, viz., for both positive and negative pitch g loads on the pilot:

$$[\text{PST-TVFC-}G_z\text{-loads}] < [\text{Conv.-}G_z\text{-loads}]$$

$$[\text{Cf. lower graphs in Fig. 3}] \quad (19b)$$

4) Adding tangential and centrifugal accelerations on a pilot situated ahead of CR does not change these general conclusions, even for the fastest measured PST-TV flip-up/down.

5) Maximum pitch-agility is affected by airframe/engine structural g limitations at high subsonic speeds, and is hardly, if at all, influenced by pilot tolerances at low speeds.

G_x during this SACOM includes positive (blood flow to chest) centrifugal acceleration acting on the pilot from CR. The G_z , G_y , G_x pilot tolerances vary differently with the duration and rate of onsets. Therefore, combined with such (a priori known) duration/rate limitations, the measurement envelopes translate into forbidden human space-time agility domains for supermaneuvers.

These domains have not yet been fully explored. Their boundaries vary, inter alia, with the distance from the pilot's head to the so-called pseudoinstantaneous CR during different, rapid supermaneuvers. Understanding these complex rigid-body translational, rotational, gyration, and gyroscopic phenomena requires reassessment of a few, well-established, human systems/aircraft/control/effectiveness concepts. Verification of such theoretical criteria, by collecting well-defined

flight-tested data can, therefore, help the design of new centrifuge simulations^{8,9} of human systems exposed to extreme PST-TV conditions, and, consequently, to establish the optimal location of the pilot's seat/head in superagile CFC-TVFC fighters.

Maximized Angular Rates

AGA angular rates (AR), namely aircraft pitch, roll, and yaw rates are, by Eq. (8), related to ideal (high-density) model angular rates via

$$\text{AGA}[\text{ARR}] = \text{MGA}[\text{ARR}][L]^{-0.5}F_1[\text{Turb.-MLEM}] \times F_2[\text{PDT/FDT}]F_3[A\text{-IFPC}]/[M\text{-IFPC}] \quad (20)$$

where aircraft vs model geometric and performance angles remain invariants and (agility) time is compressed by the factor $[L]^{-0.5}$.

The maximum (gross) pitch rate observed so far with our $\frac{1}{2}$ scale flying, low-density PST-TV-F-15 model is 175 deg/s (Table 1). It was obtained by combined TVFC and conventional elevator pitch-only commands. By (8), (20), and DIP adjust, it transforms to 70 deg/s for the full-scale fighter. For full-scale conventional F-15, the maximum obtained was 22 deg/s, and for vectoring-only command, 39 deg/s.

The measurements of G_z , G_y , G_x envelopes, and of forbidden human space-time domains for each of these upgrades, the verification of the radius of gyration methodology for the new SACOMs, and the development of mathematical approximation methods are sponsored by the USAF/AFOSR/EOARD, United Kingdom. Table 1 data for the full-scale aircraft can be employed by the Armstrong Laboratory at Wright-Patterson AFB, Ohio, and by the Human System Division at BAFB, Texas. Currently, there is no other source for the measurement of such PST-TVFC data by fast-rotating F-15, F-16, and F-22 models, or the full-scale vehicles.¹⁵

First Thrust Vectoring Rule

All our flight tests indicate that maximum agility is extractable when TVFC is properly combined with CFC. Proper CFC-TVFC combination means that the jet-rotation rates should not lag behind the maximum rotation rates extractable from advanced conventional elevators, rudders, and ailerons. Therefore, effective TVFC rates cannot lag behind the conventional ones. This is a basic effectiveness rule that can affect the future of vectored aircraft, for it forces the selection of the most effective TV nozzles and TVFC modes for proposed new or upgraded TVFC fighter aircraft.

To quantify and gauge this rule, one may first examine the time derivatives of Eq. (10). For instance, the time derivative of pitch jet deflections δ , affect the second time derivatives of the pitch rate, and hence, the pilot's ability to stop or reverse rapid, unwanted, or wanted turning rates/oscillations under conventional or PST conditions. This may help gauge the pilot's ability to minimize offensive or defensive delay times with TVFC.

Therefore, success criteria in air-to-air and in air-to-ground TVFC, or under STOL or spin-avoidance-recovery conditions, include super-fast-responding yaw-pitch, or yaw-pitch-roll rectangular nozzles.^{1,15} Consequently, such engine nozzles are being developed in this laboratory (by means of contracts with Pratt and Whitney).

Concluding Remarks

1) Fundamental concepts and integrated similarity rules for agile, PST-TVFC aircraft have been defined and employed in the construction of a unified methodology for integrating

theory with jet propulsion and flight tests of powered, PST, TVFC prototypes/models.

2) Net agility and new integrated similarities have been combined with a cost-effective SACOM testing methodology introduced via flying rotating-translating, powered, PST-TVFC F-15, F-16, and F-22 models. Forbidden human space-time domains that infer far-reaching consequences for superagile fighters are analyzed.

3) A basic PST-TVFC rule regarding the maximization of jet deflections rates has been introduced. Emulation of full-scale performance by flying low-density PST-TVFC models appears to be more productive and cost-effective than the use of wind-tunnel or unpowered/unvectored free-flying or drop models.

Acknowledgments

Part of this research has been financially sponsored by the USAF Office of Scientific Research, European Office for Aviation Research and Development, United Kingdom, under Grant Air Force Office for Scientific Research 89-0445, and Special Project SPC-91-40003. The U.S. Government is authorized to reproduce and distribute reprints for Government purposes notwithstanding any copyright notation thereon. Additional financial support has been provided by General Dynamics, General Electric, Teledyne CAE, and Pratt and Whitney, whose regulations prevent us from providing additional technical details and drawings.

References

- ¹Gal-Or, B., *Vectored Propulsion, Supermaneuverability and Robot Aircraft*, 1st ed., Springer-Verlag, New York-Heidelberg, 1990, 1991, pp. 1-257.
- ²Gal-Or, B., "The Fundamental Concepts of Vectored Propulsion," *Journal of Propulsion and Power*, Vol. 6, No. 6, 1990, pp. 747-757.
- ³Gal-Or, B., "Maximizing Post-Stall, Thrust-Vectoring Agility and Control Power," *Journal of Aircraft*, Vol. 29, No. 4, 1992, pp. 647-651.
- ⁴Gal-Or, B., "Tailless Vectored Fighters," Flight Dynamics Directorate, Wright-Patterson AFB, U.S. Air Force/Air Force Office of Scientific Research, 89-0445, July 15, 1991.
- ⁵Baumann, D. D., "F-15B High-Angle-of-Attack Phenomena and Spin Prediction Using Bifurcation Analysis," M.S. Thesis, Air Force Institute of Technology, Wright-Patterson AFB, OH, Dec. 1989; AFIT/GAE/ENY/89D-01.
- ⁶Herrick, P., "Fighter Aircraft Affordability, Survivability and Effectiveness Through Multi-Function Thrust-Vectoring Nozzles," *Intern. J. Turbo & Jet Engines*, Vol. 9, Jan. 1992, pp. 1-15.
- ⁷Goldstein, H., *Classical Mechanics*, 2nd ed., Addison-Wesley, Reading, MA, 1981, pp. 202, 203.
- ⁸Repperger, D. W., "Minimum Coriolis Algorithms for Motion Control," Armstrong Lab., Wright-Patterson AFB, OH, 1990.
- ⁹Repperger, D. W., "A Study of Supermaneuverable Flight Trajectories Through Motion Field Simulation of a Centrifuge Simulator," *J. Dyn. Meas. and Control* (to be published).
- ¹⁰Gal-Or, B., and Sherbaum, V., "Thrust Vectoring: Theory, Laboratory and Flight Tests," *Journal of Propulsion and Power*, Vol. 9, No. 1, 1993, pp. 51-58.
- ¹¹Chambers, J. R., "Status of Model Testing Techniques," Air Force Flight Dynamics Lab./ASD Stall/Post-Stall/Spin Symposium, Wright-Patterson AFB, OH, Dec. 1971.
- ¹²Woodcock, R. J., "Some Notes on Free-Flight Model Scaling," Air Force Flight Dynamics Lab. TM-73-123-FGC, Wright-Patterson AFB, OH, Aug. 1973.
- ¹³Stuart, J. L., Segal, B. D., and Bowser, C. H., "Conduct and Results of YF-16 RPRV Stall/Spin Drop Model," Air Force Systems Command, Air Force Flight Test Center, TR-76-42 Edwards AFB, CA, April 1977, pp. 18, 19.
- ¹⁴Chambers, J. R., and Illif, K. W., "Estimation of Dynamic Similarity Parameters from Drop Model Flight Tests," Air Force Dynamics Lab./Wright-Patterson AFB, Dayton, OH, 1981.
- ¹⁵Gal-Or, B., "Vectored F-15 and F-22," Report to USAF-AFOSR-EOARD, Rept. SPC-91-4003, London, UK, Aug. 1992.